Landslides of the 1920 Haiyuan Earthquake, northern China

Yueren Xu [1,3,*], Jing Liu-Zeng [2], Mark B. Allen[3], Weiheng Zhang[1], Peng Du [1]

1. Key Laboratory of Earthquake Prediction, Institute of Earthquake Forecasting, China Earthquake Administration, Beijing, China 100036

2. Institute of Surface-Earth System Science, Tianjin University, Tianjin, China 300072

3. Department of Earth Sciences, Durham University, South Road, Durham, DH1 3LE, UK

*** Corresponding E-mail: xuyr@ief.ac.cn**

Abstract The great M~8 1920 Haiyuan earthquake (HYEQ) was one of the largest and most deadly earthquakes in China in the last century, with ~234,000 deaths. The earthquake occurred within the Loess Plateau of northern China, where Quaternary loess deposits form a distinctive blanket across the landscape. Large regions of this loess cover experienced co-seismic landslides. Based on an analysis of the original disaster reports, field surveys, and satellite image interpretation, we have compiled the shaking effects of the earthquake, including the distribution of landslides, fatalities, and structural damage. Landslides triggered by the HYEQ (n >7,000) are concentrated south of the Haiyuan Fault, in a region that has both thick loess cover and long-term relief generated by the drainage network. This distribution is spatially separate from landslides triggered by other earthquakes. We find that in contrast to previous studies, the most important factor in the severe death toll of the HYEQ was the collapse of housing by ground shaking, including collapse of loess house-caves. Landslides were a secondary factor; although up to 32,000 deaths occurred in areas with intense landsliding. Based on the revised distribution pattern of landslides and damage (e.g. house collapses), we suggest that the isoseismal intensity IX line extends south of previous locations. We have also identified 126 dammed lakes created by co-seismic landslides, which form major modifications of this semi-arid landscape. The research methods in this paper, combining historical review, satellite image interpretation and field validation of landslides, can be used as a reference for studies of other areas affected by historical earthquakes and co-seismic landslides, elsewhere in the Loess Plateau and beyond.

Keywords 1920 Haiyuan Earthquake; landslide; historical damage report; Loess Plateau

1 Introduction

Unlike earthquakes that occurred in recent times, historical earthquakes and co-seismic landslides are poorly understood. Recent earthquakes, such as the Wenchuan earthquake of M_w 7.9 on May 12 2008 in Sichuan Province, China, are rapidly studied, including the seismology, surface ruptures, landslides, and effects on the regional population (Yin et al., 2009; Huang et al., 2009). Information on historical earthquakes and their effects is based on records in non-scientific literature. Many of these documents did not follow scientific procedures and the contents were brief and short. This may lead to overestimation or underestimation of the real extent of the disaster.

Historical strong earthquakes need to be studied using modern technologies to assess previous understanding of earthquake rupture and ground shaking based on qualitative descriptions, because appropriate earthquake parameters have a significant impact on regional seismic hazard assessment (Liu-Zeng, et al., 2015). Like research on modern earthquakes, detailed investigation of surface ruptures and earthquake-triggered landslides for historical earthquakes is important to determine (or revise) their parameters, including magnitude, isoseismal maps and recurrence interval.

Previous studies have shown that the spatial distribution of co-seismic landslides can be a good indicator of the earthquake rupture area and extent of co-seismic shaking (Yuan et al., 2013; Parker et al., 2011). Here, we study the effects of the Haiyuan Earthquake, using abundant literature records, the nature and distribution of earthquake-triggered landslides, and estimates of damage using comprehensive remote sensing interpretations. In particular, we carried out a spatial analysis of contemporary accounts of the effects of the earthquake, using information previously only collated in table format within somewhat inaccessible literature (e.g. Lanzhou Institute of Seismology, SSB, et al., 1980).

The Ningxia Haiyuan great earthquake (or simply, the Haiyuan earthquake) occurred on December 16, 1920. The Haiyuan earthquake killed at least 234,000 people (Lanzhou Institute of Seismology, SSB, et al., 1980). It was accompanied by a 240-km long surface rupture zone on the seismogenic fault - the left-lateral strike-slip Haiyuan fault (Deng et al., 1990; Zhang et al., 2005). The coeseimic horizontal offset reaches a maximum of 10 m (Deng et al., 1990; Zhang et al., 2005), and ~5 m on average (Ren et al., 2016). The exact magnitude of the earthquake is not fully resolved. Although commonly quoted as high as *M* ~8.5, a value of *M* 7.8 seems more realistic based on the rupture parameters (e.g., Liu-Zeng, et al., 2015). The earthquake triggered a large number of landslides (Lanzhou Institute of Seismology, SSB, et al., 1980; Zhuang et al., 2018; Li et al., 2015) (Fig. 1), which exacerbated deaths and caused considerable changes in local landscapes.

Landscape and landslide analysis in the Haiyuan region is complicated by the existence of the 1718 Tongwei earthquake (*M* ~7.5), with an epicentre ~160 km to the south of the Haiyuan event. This event highlights a problem around assessment of historical earthquakes: which landslides were triggered by the Haiyuan earthquake, and which had already been in existence for more than 200 years, and were triggered by the Tongwei earthquake? More generally, what are the spatial distributions of landslides and other effects of these two strong earthquakes? These landslides undoubtedly had disastrous human consequences in each earthquake, but the full extent is important to clarify. For example, it has been claimed that the Haiyuan earthquake killed >100,000 people via co-seismic landslides (Derbyshire et al., 2001), but this figure has not been re-evaluated.

Because of the age of the Tongwei earthquake, the available literature is scarce and lacks detail (Lanzhou Institute of Seismology, SSB, 1989), whereas the records of the Haiyuan earthquake are relatively rich, the spatial coverage is larger, and there are relatively detailed statistics of the disasters faced by towns and villages (Lanzhou Institute of Seismology, SSB, 1989; Seismological Bureau of Ningxia Hui Autonomous Region, 1989). These datasets are rich background information for this study. We use them alongside catalogues of co-seismic landslides (Xu et al., 2020), derived from high-resolution satellite imagery and fieldwork.

Based on a review of the literature records, field surveys, and detailed visual interpretation of Google Earth images, we have recently published a catalogue of landslides (Table 1), which covers>67,500 km^2 on the northeastern of the Tibetan Plateau (Figure 2), in the vicinity of the Haiyuan earthquake (Xu et al., 2020). This landslide database contains 7,151 individual landslides (Table 1). The landslide catalogue contains spatial location information and corresponding attribute information, including area, length, width, trailing edge elevation, leading edge elevation, and height. Based on the literature records, the distribution and characteristics of the Haiyuan earthquake landslides are discussed. Then, we detail the role of historical earthquake landslides in the spatial distribution of earthquake damage. We also discuss adjustments to the isoseismal map of the Haiyuan earthquake.

2 Historical information on the Haiyuan earthquake

2.1 Background and methods

Starting four months after the Haiyuan earthquake, on April 15, 1921, six Chinese scholars, Dr. Weng WenHao, Xie Jiarong, Wang Lie, Su Benru, Yi Shoukai, and Yang Jingwu from Beijing conducted a 4-month post-earthquake scientific investigation. They started their trip from Lanzhou, passed Huining and Jingning to Guyuan, and then returned back via Pingliang and Tianshui (Fig. 1a). They collected information regarding the disaster situation through field surveys and questionnaires for the local government (Table 2). The relevant survey results were then published through newspapers and special reports, summarized in the 1980s in Lanzhou Institute of Seismology, SSB, (1989), and Seismological Bureau of Ningxia Hui Autonomous Region, (1989). This fieldtrip was the first comprehensive and detailed scientific investigation of a strong earthquake by Chinese scientists in mainland China (Lanzhou Institute of Seismology, SSB, et al., 1980; Gu, 1983).

Fig. 2 shows the spatial distribution of major historical strong earthquakes in the study area, and the commonly used intensity map of the Haiyuan earthquake (Department of Earthquake Disaster Prevention, SSB, 1995). We matched ancient and modern place names individually, and the disaster information at specific points is displayed in map form, to show regional differences in the extent of the disaster.

Data used in this study for deaths, house collapses and livestock losses were mainly obtained from books published decades after the disaster, that compiled reports made in the immediate aftermath: Summary of Gansu Historical earthquake Record (Lanzhou Institute of Seismology, SSB, 1989), and Summary of Ningxia Hui Autonomous Region Historical Earthquake Record (Seismological Bureau of Ningxia Hui Autonomous Region, 1989). Through the comparison and verification of the tabulated data in these different data sources, we obtained new distribution maps of deaths caused by the Haiyuan earthquake (Fig. 3), collapsed houses (including caves) (Fig. 4), the deaths of livestock (cattle, horses, and mules) (Fig. 5), and the number of co-seismic landslides reported as "Cracked Mountains" (Fig. 6). In each case we have converted the point count data of the original reports into contour maps, showing the density distribution of each parameter, using the kernel intensity method in ArcGIS with a searching parameter of 50 km. Most of the original data were recorded in terms of a number per locality, which makes a density analysis feasible. A ~100 x 100 km region west of Xiji recorded data in percentage format, which is not readily comparable with the rest of the data (Fig. 4 and Fig. 5).

2.2 Literature data

The death toll from the Haiyuan earthquake was concentrated in eight counties: Haiyuan, Guyuan, Longde, Jingning, Huining, Tongwei, Jingyuan, and Xiji (Table 2, Fig. 3). A total of 198,861 people died in these counties (Lanzhou Institute of Seismology, SSB,1989; Seismological Bureau of Ningxia Hui Autonomous Region,1989) accounting for ~85% of the total. Xiji County was established in 1942, 22 years after the Haiyuan earthquake (Xiji County Annals Compilation Committee, 1995), through the merger of parts of Longde, Guyuan, and Haiyuan counties. The statistical analysis in this study is based on the original seven counties.

Fatalities were worst in the eastern and southern counties. Haiyuan County had the largest number of deaths (>73,000) (Haiyuan County Annals Compilation Committee, 1999), accounting for 59% of its population, including 4,334 deaths in Haiyuan County township (Table 2). Various towns had death tolls of >1,000 in Longde, Jingning and Guyuan counties (some of them now in Xiji County) (Fig. 3). The number of deaths in Jingtai and Jingyuan was relatively small, because they are located in landscapes of the Gobi Desert to the north of the Loess Plateau, which have sparse populations. However, mortality rates reach >70% in individual settlements (Lanzhou Institute of Seismology, SSB, et al., 1980).

Outside the southern part of intensity zone IX, there are townships with death tolls in the hundreds (Regions A and B in Fig. 3), i.e., south of Tongwei to Tianshui. The number of deaths gradually decreased away from the epicenter from hundreds to tens, to only a few (Regions B and C in Fig. 3). In addition, from Pingliang to Qingyang, although the number of deaths in some larger individual townships was close to 1,000 because of their population density, overall death rates (<10%) were smaller than those in Haiyuan or Guyuan (Region D in Fig. 3).

The number of collapsed houses caused by the Haiyuan earthquake (Fig. 4) is only partly consistent with the distribution of deaths (Fig. 3). Types of residential houses are both conventional brick houses and loess caves ("Yaodong" in Chinese); neither had earthquake resilience features. The Haiyuan County Town had a >90% building collapse rate; there are no specific statistics for deaths caused by collapse rather than other mechanisms (Lanzhou Institute of Seismology, SSB, 1989). The number of collapsed houses in each town of Xiji, Longde, and western Guyuan reached approximately ~1000. House collapse rates in Jingyuan and Huining were 50-90%, including some sites outside of intensity zone Ⅸ (Fig. 4) (Lanzhou Institute of Seismology, SSB, 1989). Damage statistics for the above areas are consistent with the high death tolls in the same areas (Fig.s 3 and 4). But, the density distribution for collapsed houses gives an apparent high in the Tongwei region, which is not consistent with the relatively low death toll in the same area (Fig. 4). South of Tongwei to Tianshui, the number of collapsed houses decreased from ~1000 to ~100; the situation in Pingliang to Qingyang was similar (Fig. 4). It should be noted that around low-intensity areas, some of the statistics for collapsed houses may include less serious damage, resulting in an increase in the number. This conclusion is based on our analysis of field survey photos of Tianshui (Lanzhou Institute of Seismology, SSB, et al., 1980). In general, from south of Tongwei to Tianshui and east of Pingliang to Qingyang were less affected areas (Regions B and C in Fig. 4).

The overall spatial distribution of large livestock deaths caused by the Haiyuan earthquake was partly consistent with the number of human deaths (Fig.s 3 and 5). The numbers of livestock deaths in the epicentral region reached ~10^4-10^5 in individual towns. The death rate between Jingyuan and Tongwei was mostly 60-80%, and even went up to 90%, while the number of livestock deaths outside the epicentral region dropped sharply to ~10^3 or ~10^2, showing an order of magnitude attenuation. Due to the statistical table issued at the time, the term "livestock" is not strictly defined and abnormal livestock deaths occurred in some towns. These numbers may include the deaths of small livestock such as sheep and goats. For example, Jingtai, with relative small population, recorded ~10^5 livestock deaths. This is obviously the result of adding data for smaller animals. The area is part of the Gobi, where sheep are more prevalent than large livestock. Between Jingyuan and Tongwei there was a similar distribution of deaths inside and outside of intensity zone IX, with a death rate of 50-90% (Fig. 5), which is consistent with the data for human deaths and collapsed houses (Fig.s 3 and 4).

Disaster investigators designed an entry called "Cracked mountains" for the disaster survey form (Table 3) (Lanzhou Institute of Seismology, SSB, 1989). These features are landslides triggered by the Haiyuan earthquake, mapped in Fig. 6. The sites are concentrated in Xiji, Jingning, Huining and Longde counties, and are located to the south of the Haiyuan Fault. There are only a few reports near Tongwei, and only 7 cases were reported south of Tongwei. Near Pingliang, there are only 4 cases. These recorded landslides are mainly related to intensity zones IX and X. Some of them are outside intensity zone IX; for example, south of Jingning County there are 45 cases in a small area (Region A in Fig. 6). There are more than 10 cases in sites around Xiji County. Despite the large number of landslides within the epicentral area, some towns and villages did not report landslide events because the high death toll inhibited responses. The co-seismic landslides reported here mostly refer to the most significant landslides, including those that caused a village to be buried. A large number of landslides scattered in gullies were not taken seriously by the people at that time, which led to a large number of landslides not being covered in surveys after the earthquake.

3 Results from remote sensing and fieldwork

3.1 Methods

The landslide dataset utilized in this study was originally presented in Xu et al (2020), so only brief details of the survey methods and assumptions are given here. The Haiyuan earthquake epicentral area and surrounding areas were interpreted systematically using high-resolution satellite images from Google Earth. Image analysis was supported by fieldwork in

2015-2019 in these areas to provide “groundtruthing”. Digital elevation models (DEM) were constructed for more than 20 sites, using unmanned aerial vehicles (UAV). Field surveys found that the Haiyuan earthquake-triggered landslides are mainly within loess sediments; the loess forms a blanket layer over much of this part of northern China. There are fewer landslides that involved bedrock under the loess (Lanzhou Institute of Seismology, SSB, et al., 1980; Lanzhou Institute of Seismology, SSB, 1989; Seismological Bureau of Ningxia Hui Autonomous Region, 1989). The images were cross-checked at least 3 times, including against US Keyhole satellite images of 1960s–1970s vintage. Systematic interpretations and landslide identifications were performed on a basin-by-basin series. Two aspects of the survey need highlighting. First, rainfall-generated landslides were eliminated on the basis of similarities with landslides known to have been generated in the 2010 storms in the Tianshui region (small area and shallow depths; see Xu et al., 2020). Second, there is the problem that we cannot determine the age of every landslide. There is the possibility that a proportion of the mapped landslides were not generated in 1920, but in fact are relict in the landscape from earlier earthquakes. More subtly, we do not know how many landslides took place in 1920 by reactivation of pre-existing scarps. We have addressed this problem by studying individual landslides that are clearly identified as having taking place in 1920, from original eye-witness reports. The characteristics of these landslides are used as benchmarks for the identification of other landslides in the same region. Characteristics include dimensions, but also the degree of landslide visibility in the landscape, which is expressed by the sharpness of the headwall and marginal scarps. It is also useful information where eye-witness reports after the 1920 Haiyuan earthquake did not identify fresh landslides, especially where there are landslides present in the landscape. Such landslides are more robustly related to previous earthquakes.

During the interpretation of the Haiyuan earthquake using Google Earth imagery, the boundaries of the targeted landslides were extracted using a vector file. Each extracted landslide was cataloged and sorted according to the date and saved as a *.kml file. The attribute information of the landslide body was assigned in the ArcGIS Software. The attribute information includes the longitude and latitude of the center point of the landslides, their length and width, the trailing edge elevation, and leading-edge elevation. We can also obtain the height of the landslides according to the latter two measurements. After the initial interpretation was completed, we conducted random checks on the primary results to ensure accuracy and reliability.

3.2 Results of remote sensing and mapping

We mapped 7,151 landslides in the vicinity of the Haiyuan earthquake epicentre (Xu et al., 2020), and here present an analysis of their distribution and characteristics. Regions of high landslide density are distributed in multiple scattered patches (Fig. 2), instead of being concentrated adjacent to the Haiyuan Fault. Landslides are concentrated in the eastern section of the Haiyuan Fault, while western sections have lower numbers (Fig. 2). There are more landslides on the south side of the Haiyuan Fault than on the north side (Fig. 2).

Areas with dense concentrations of landslides in the vicinity of the Haiyuan earthquake can be defined into 8 regions (Fig. 10). Regions A and C are located along the Haiyuan Fault. The famous Lijunbao Landslide is located in Region C (Fig. 10), where the co-seismic surface rupture also passed near the site (Lanzhou Institute of Seismology, SSB, et al., 1980; Deng et al., 1990). Region B is located southwest of Xiji. Landslide-dammed lakes are located in this region, including the Dangjiacha dammed lake (Figs. 7 and 8). Region H is located west of Jingning, which covers the main roads connecting Guyuan, Pingliang, Tianshui, and Lanzhou (Fig. 1), so the landslides in this region were recorded by the post-earthquake scientific research (Lanzhou Institute of Seismology, SSB, et al., 1980) and international rescue workers (Close and McCormick, 1922) in 1921. These eye-witness accounts provided valuable information and photographs to assist our interpretation of landslides triggered by the Haiyuan earthquake. Region G is located northwest of Longde. Regions D, E, and F are located near Guyuan, on the northeast side of the Haiyuan Fault.

Landslide numbers are projected onto two profiles, roughly parallel and perpendicular to the Haiyuan Fault, on Fig. 9. These profiles show the concentration of co-seismic landslides east of the Haiyuan earthquake epicentre, and south of the Haiyuan Fault. There is a decline in the number of landslides southwards, before a high-density area of landslides attributed to the 1718 Tongwei earthquake.

We used Google Earth to extract the locations of the main residential areas in the study area. Settlements were rebuilt on or near the ruins after the 1920 earthquake (Lanzhou Institute of Seismology, SSB, et al., 1980). Therefore, the current distribution of settlements largely represents the distribution of settlements during the earthquake (Fig. 10). The distribution of settlements is sparse on the northwest side of Haiyuan Fault (mainly distributed along the fluvial terraces of the Yellow River), dense on the southeast side, sparse on the north side (concentrated along river valleys), and dense on the south side.

Combining the data for the landslides and the settlements, it is clear that the five dense landslide regions to the south of the Haiyuan Fault are also areas with high settlement density. In these regions, landslides aggravated the number of casualties and the loess of property (Fig. 10; Close and McCormick, 1922). Settlements in Regions D and F are relatively sparse, so the landslides did not cause the same loss as in the above regions. Deaths in regions D and F were mainly caused by houses collapsing, including Yaodong collapse (Close and McCormick, 1922). A large number of people also died in the settlements around Haiyuan (~66,000), mainly due to the collapse of Yaodongs and conventional houses (Fig. 10).

Fig. 10 also shows regions further away from the Haiyuan earthquake epicentre, where we have recorded landslides (Xu et al., 2020), but consider that other earthquakes were the triggers. Region M, located south of Tongwei, is densely populated; the residential areas within this region suffered severe damage during the Tongwei earthquake, which caused more than 70,000 deaths (Table 1, Fig. 2, Fig. 10, Xu et al., 2020). Region K is located between Qin'an and Tianshui, which coincides with the epicenter of the AD 734 Tianshui earthquake. Settlements affected by this earthquake suffered serious death tolls (Lei et al., 2007). We are able to estimate the extent to which Tongwei earthquake landslides were reactivated during the Haiyuan earthquake. There are only five reported landslides in the Tongwei region (Fig. 6) caused by the Haiyuan earthquake, indicating that the new movement was limited, and not a widespread threat to life or property in this region. The main cause of deaths in the Tongwei area due to the Haiyuan earthquake were house collapses and the freezing weather during the winter of 1920/1921 (Table 2; Tongwei County Annals Compilation Committee, 1990).

Combining the literature records and the remote sensing identifications (Table 2; Fig. 3, Fig. 10), we summarize the landslide and death tolls for different regions (Table 5). The total number of landslides in the above 8 regions is 5,276, accounting for 73.7% of the total number identified by Xu et al (2020) in the vicinity of the Haiyuan earthquake. The corresponding death toll of or the same areas is 32,554. Although some deaths may be missing from the reports in the dense landslide regions, according to the data that are available, we can be confident that the death toll was >32,000. Not all deaths in the residential areas were necessarily caused by landslides, so our results do not support the view that more than 100,000 people died because of landsliding in the 1920 earthquake (Derbyshire et al., 2001; Wang et al., 2003).

According to the available statistics, the factor that caused the most deaths in the Haiyuan earthquake was the collapse of houses and loess cave houses, through strong shaking, e.g. the Haiyuan county township had more than 4,000 deaths and is located on an alluvial fan (Table 2). Post-earthquake scientific investigations reported some local settlements buried by landslides along the main roads (Close and McCormick, 1922; Lanzhou Institute of Seismology, SSB, et al., 1980), which magnified the impact of co-seismic landslides, even it is true that they were fatal and devastating under certain conditions (Fig. 10).

Fig. 11 shows two images of Haiyuan County town, taken in 2018 and 1970, i.e. nearly 100 and 50 years after the 1920 earthquake, respectively. Rebuilding after the earthquake followed the pre-earthquake street patterns and used similar construction methods; the image from 1970 shows a town little changed in extent from 1920, with the original mass grave still located near the edge of town. By 2018 (the date of the satellite image in Fig. 11a), urban growth had greatly extended the limits of the town, but much of the building used modern construction methods. The rural villages rebuilt their houses in the traditional style, without frame structures, even though the walls were rebuilt by sintered bricks. Most of these buildings weak resistance to earthquake shaking (Fig. 12).

Loess landslides blocked river valleys, forming dammed lakes (Close and McCormick, 1922) (Figs. 7, 8 13 and 14). There are 49 well-preserved earthquake-dammed lakes in the Haiyuan region identified in our dataset. There are other 33 relict earthquake-dammed lakes, where the water has dried up and/or the lake has silted up, as shown in Figs. 13, 14. Some dammed lakes were drained after the landslide dam was breached or overtopped. In addition, there are another 44 dammed lakes which were used as reservoirs after artificial modification. These earthquake-dammed lakes in different states show the modification process of landslides related to the Haiyuan earthquake under natural and human activities in the past 100 years (Figs. 13, 14). Fig. 7 includes the epicentral region of the 1970 *M* ~5.5 Xiji earthquake, and shows how this moderate sized earthquake did not produce significant modification of the landscape in this region, including changes caused by the Haiyuan earthquake such as dammed lakes.

The total number of landslides in the 2008 Wenchuan earthquake catalogue is much larger than the Haiyuan catalogue, and nearly equivalent (Table 1) to the number in the Tianshui rainfall landslide catalogue Xu et al (2020). Therefore, it is clear that a large number of co-seismic landslides of area ≤10^4 m^2 are missing from the Haiyuan catalogue, because of their smaller scale, shallow-seated nature, and tendency to be easily altered and lost by human activity or surface vegetation recovery (Xu et al., 2020). These large numbers of "disappeared" landslides contribute little to the total landslide volume, however. Although the Haiyuan catalogue is therefore an incomplete database, the landslides in the area range of ≥10^4 m^2 determines the overall characteristics of the earthquake-triggered landslide catalogue, accounting for about 80% of the total area, and 60% of the volume.

4 Discussion

The distribution of earthquake-triggered landslides is controlled by three factors: the nature of the original rupture (dimensions and energy released), local geological and geomorphic conditions (nature of the substrate, pre-existing relief), and elapsed time (Yin et al., 2009; Yuan et al., 2013; Xu et al., 2014). There are completely different distribution characteristics of earthquake-triggered landslides on each side of active dip-slip faults (Xu et al., 2018). Landslides triggered by thrust-type earthquakes tend to be more concentrated on the hanging wall, while landslides triggered during normal faulting tend to be on the uplifted footwall block (Liu, 1984; Xu et al., 2014; Xu et al., 2018). Landslides are often densely distributed along both sides on both sides of strike-slip faults (Xu et al., 2014). However, specific geological and geomorphic conditions will change the distribution characteristics from expectations.

The Haiyuan Fault is a left-lateral strike-slip fault. For large distances along its length, the landscape has low relief and characterized by fluvial and alluvial Quaternary deposits, with no significant slopes for landslides. These areas only experienced large-scale ground fissures during the Haiyuan earthquakes (Lanzhou Institute of Seismology, SSB, et al., 1980). For example, the roads connecting Haiyuan County Town to the Dry Salt Ponds, Guyuan, and Zhongwei were disrupted by dense fissures, but no large-scale dense landslides were reported (Lanzhou Institute of Seismology, SSB, et al., 1980).

The region south of the Haiyuan Fault, east of the Yellow River, north of the Wei River, and west of Liupanshan, is typical hilly, with thick loess deposits, which can cause a large number of loess landslides during the shaking process (Fig. 6), but the interpreted landslide distribution is focused at the Haiyuan-Guyuan-Xiji-Jingning area, and the number of landslides 100 km away from the Haiyuan Fault decreases sharply (Fig.s 2, 6, and 10). The number of co-seismic landslides on both sides of the fault zone westward from Haiyuan to Jingtai is very small, and this area is dominated by bedrock mountains and the Gobi Desert. Except for sand liquefaction on the Yellow River terraces, it is not optimal for generating landslides in this region (Fig. 2). In addition, the possibility cannot be ruled out that the shaking in the western part of the rupture was less strong. These factors contribute to the overall pattern that the spatial distribution of Haiyuan earthquake landslides is uneven, and clustered (Fig. 2), with more common landslides in the higher relief, loess-covered areas on the south side of the Haiyuan Fault than the lower relief, Gobi Desert region to the north. Fig. 10 highlights how landslides are concentrated along some of the main river valleys of the region, especially the Qingshui River which flows north into the Yellow River. These regions contain the combination of loess sediments, but also relief, such that shaking triggered landslides on valley slopes, moving towards the local valley floor.

Comparison of Figs. 2, 6 and 10 emphasizes how several regions away from the Haiyuan earthquake epicenter contain high numbers of landslides, but in each case there are few contemporary reports of landslides in 1920. These regions of high landslide density can be correlated with one or other of the older historic earthquakes, namely the AD 1718, 1654 and 734 events. This correlation emphasizes several points. First, that major landslides can persist in the Loess Plateau landscape for >1000 years – and possibly ~3000 years given the apparent concentration of landslides near the epicenter of the BC 780 Qishan earthquake (Fig. 2). This longer timeframe is similar to the recurrence interval of major earthquakes in the region, estimated at 2,000 – 3,000 years on the basis of a paleoseismicity study of the Huoshan Piedmont Fault, which is located further east (Xu et al., 2018).

We speculate that the landslide distribution be partly related to the gradual transition of the Haiyuan Fault into thrusting on the Liupanshan Fault, with the caveat that co-seismic surface ruptures have not been identified along the Liupanshan Fault. It may be more of a factor that landslides were concentrated in areas of higher relief (e.g. along the Qingshui River valley, Fig. 10), generated by the long-term regional patterns of uplift on the Liupanshan Fault and other thrusts, rather than co-seismic motion in 1920. It is also notable that landslides are concentrated within the region of loess deposition, rather than the sand and rock outcrops of the Gobi Desert to its north (Fig. 2). Fig. 10 highlights that there is a concentration of landslides in regions characterized by loess cover, proximity to the epicentre, and relief generated by long-term fluvial incision into the landscape. There is scope for future work on correlating landslide density and regional geomorphology, for application to other earthquake-prone parts of the Loess Plateau.

In the Jingyuan-Huining-Tongwei region (Fig. 2), which lies beyond the accepted location of isoseismal intensity line IX, apart from the small number of recorded landslides, the spatial distribution of earthquake damage is similar to regions with intensity >IX to the north (Figs. 3-5). The previous criteria for defining the intensity lines were mainly based on the overall disaster records of the main settlements in the counties, which provided the situation of individual townships but not the regional picture (Figs. 3-5). Therefore, we suggest that the isoseismal line of intensity IX in this area is not reasonable, and should be revised based on the reported distribution of damage as summarized in Figs. 3-5. The new suggested line extends to the southwest of the conventional position (Fig. 2).

The numerous landslides near Tongwei were triggered by the effects of the close-by Tongwei earthquake (Xu et al., 2020). The far-field effects of the Haiyuan earthquake were 202 years later, and caused localized landslides which were much less devastating than the Tongwei earthquake (Table 2). However, the post-earthquake scientific investigation (Lanzhou Institute of Seismology, SSB, et al., 1980) attributed the damage in the Tongwei region to the Haiyuan earthquake; in fact, the severity of the damage caused by the Haiyuan earthquake in this area has greatly been exaggerated, which resulted in anomalous regions of intensity X drawn by some researchers (Fig. 1c) (Lanzhou Institute of Seismology, SSB, et al., 1980).

The density distribution maps for deaths, house collapses and livestock losses are not completely consistent with each other (Figs. 3-5). The house collapse contours show an apparent high in the region between Tongwei and Gangu (Fig. 4), but we suspect this overstates the extent of the damage in this region because partial damage was recorded as complete collapse. In contrast, the relatively lighter damage reported from closer to the epicentre may reflect the extremely high death toll in this area: the dead cannot report their losses, while recording property damage was not top priority for survivors.

In future studies, epicenters that have not been determined or seismogenic faults that are not yet clear can be analyzed using landslide distribution maps and historical records. We can further broaden the study of major Holocene earthquakes by synthesis with archaeological data, which records damage in prehistoric civilizations caused by ancient earthquakes e.g. the Lajia site (Wu et al., 2016).

When conducting interpretation of historical strong earthquakes and landslides on the Loess Plateau, some points need to be considered: First, how to deal with the superposition effect of multiple earthquakes (such as the Tongwei and Haiyuan earthquakes). Our study shows how present-day data (i.e. remotely sensed images) can be combined with literature data, and compilations of eye-witness records in particular. Differences in spatial distributions should be analyzed, and the relationship between the macro-epicentral region and the causative seismogenic fault should be distinguished. Second, how to confirm aftershock effects after a major earthquake (such as, strong aftershocks within months after the Haiyuan earthquake, and later damage caused by moderately-sized earthquakes). The 1970 Xiji *M* 5.5 earthquake shows that in general moderate earthquakes have limited energy and will not change the overall spatial distribution of main landslides (Fig. 7). This is an important basis for us to carry out remote sensing research on historical strong earthquake triggered landslides. Third, some historical earthquakes and landslides that occurred a long time ago can also be studied via sediments from dammed lakes, and large-scale exploration and trenching of the trailing edge of landslides. Sampling of the trough profile, sampling of the underlying original topographical surface of the landslide, and sampling of the overlying slope deposits can accurately determine the age of occurrence of typical landslide bodies to perform comparisons with the literature. Finally, it has to be considered how unstable Haiyuan landscapes are, 100 years after the earthquake. The potential for future landslides on slopes destabilised in 1920 is an under-explored aspect of seismic risk in this area.

6 Conclusions

We have combined a review of historical reports on the damage caused by the Haiyuan earthquake with our recent survey of landslides in the area (Xu et al, 2020). Our landslide database lacks smaller landslides generated by the earthquake or by rainfall over the following 100 years. The most intense landsliding caused by the Haiyuan earthquake is concentrated in the southeast section of the Haiyuan Fault, in regions with combinations of loess sediments and relief generated by the major drainage networks (Fig. 10). Utilizing official reports of the damage and landslides made shortly after the event, we are able to separate landslides generated by the Haiyuan earthquake from clusters likely to have been generated by earlier events, such as the dense landslides around Tongwei-Gangu likely to have been triggered by the 1718 Tongwei earthquake.

Haiyuan earthquake landslides only caused direct damage to settlements or aggravated the loss of life and property in specific areas. At least 32,000 people died in landslide-dense regions, accounting for 13.6% of the total fatalities caused by the earthquake, but only a fraction of the deaths would have been related directly to landsliding even in these areas. Therefore, the most important factor causing death and injury of people is was the strong shaking that lead to the collapse of houses or the burial of loess caves.

The imbalance of engineering geology and settlements in the research area and the magnification effect of loess hills and river terraces led to the previous estimates of a "Water Drop" shape to the intensity lines of the Haiyuan earthquake. We suggest that the seismic intensity line IX to be expanded to the south of previous maps, and passes through the Jingyuan-Tongwei-Zhuanglang region, which is bigger than before (Fig. 2).

The Haiyuan earthquake landslide database given in this paper, despite lacking small and medium-sized landslides, can generally represent the overall spatial and statistical characteristics of coseismal landslides in the macro-epicentral region. The research methods of combining historical documentation and geological investigation in this paper can be used as a reference for studying other historically strong earthquakes and associated natural hazards, in regions with long written records of earthquakes.

Acknowledgements

Funding for this research was provided by the Fundamental Scientific Research Fund in the IEF, CEA grant 2019IEF0201, 2017IES010101, 2017IES010102, National Natural Science Foundation of China grant 41502204, U1839203, Seismic Active Fault Exploration Project based on High-resolution Remote Sensing Interpretation Technology by Department of Earthquake Damage Defense, CEA grant 15230003. Yueren Xu was sponsored as Academic Visiting Scholar to University of Durham by the China Scholarship Council grant 201604190021. We thank two reviewers for their constructive comments.

References

[1] Cheng J, Rong Y, Magistrale H, Chen G, Xu X (2017) An M_w-Based historical earthquake catalog for Mainland China. Bulletin of the Seismological of Society of America 5: 2490-2500. https://doi.org/10.1785/0120170102

[2] Close U, McCormick E (1922) Where the mountains walked. National Geographic Magazine 41: 445-464.

[3] Dadson S J, Hovius N, Chen H, Dade WB, Lin JC, Hsu ML, Lin CW, Horng MJ, Chen TC, Milliman J, Stark CP (2004) Earthquake-triggered increase in sediment delivery from an active mountain belt. Geology 8: 733-736. https://doi.org/10.1130/G20639.1

[4] Department of Earthquake Disaster Prevention, SSB (1995) Catalogue of Historical strong earthquake in China. Seismological Press (in Chinese), Beijing

[5] Derbyshire E (2001) Geological hazards in loess terrain, with particular reference to the loess regions of China. Earth-Science Reviews 1-3: 231-260. https://doi.org/10.1016/S0012-8252(01)00050-2

[6] Du P, Xu YR, Tian QJ, Zhang WH, Liu S (2020) The spatial distribution and attribute parameter statistics of landslides triggered by the May 12th ,2008, M_w 7.9 Wenchuan Earthquake. Earthquake Research in China 34(1): 120-141. https://doi.org/10.19743/j.cnki.0891-4176.202001006

[7] Gu GX (Ed) (1983) Catalog of Chinese Earthquakes (BC 1831-AD 1969). Science Press (in Chinese), Beijing

[8] Guyuan County Annals Compilation Committee (1993) Guyuan County Records. Ningxia People Publishing House (in Chinese), Yinchuan

[9] Haiyuan County Annals Compilation Committee (1999) Haiyuan County Records. Ningxia People Publishing House (in Chinese) , Yinchuan

[10] Huang RQ, Li WL (2009) Analysis of the geo-hazards triggered by the 12 May 2008 Wenchuan Earthquake, China. Bulletin of Engineering Geology and the Environment 68(3): 363-371. https://doi.org/10.1007/s10064-009-0207-0

[11] Huining County Annals Compilation Committee (1994) Huining County Records. Gansu People Publishing House (in Chinese), Lanzhou

[12] Jingning County Annals Compilation Committee (1993) Jingning County Records. Gansu People Publishing House (in Chinese), Lanzhou

[13] Jingyuan County Annals Compilation Committee (1995) Jingyuan County Records. Gansu Cultural Publishing House (in Chinese) , Lanzhou

[14] Lanzhou Institute of Seismology, SSB, Seismic Crew of Ningxia Hui Autonomous Region (1980) AD 1920 Haiyuan great earthquake. Seismological Press, Beijing

[15] Lanzhou Institute of Seismology, SSB (1989) Summary of Gansu historical earthquake record. Seismological Press (in Chinese), Beijing

[16] Larsen I J, David R M, Oliver K (2010) Landslide erosion controlled by hillslope material. Nature Geoscience 4: 247-251. https://doi.org/10.1038/ngeo776

[17] Li W, Huang R, Pei X, Zhang X (2015) Historical co-seismic landslides inventory and analysis using Google Earth: a case study of 1920 M 8.5 Haiyuan earthquake, China. In Engineering Geology for Society and Territory. Springer, Cham 2: 709-712. https://doi.org/10.1007/978-3-319-09057-3_118

[18] Liu BC (1984) An interpretation of the aerial photographs of the earthquake areas for Tongwei earthquake in 1718 and Tianshui earthquake in 1654. Journal of Seismological Research (in Chinese) 1: 1-7

[19] Liu-Zeng J, Shao Y, Klinger Y, Xie K, Yuan D, Lei Z (2015) Variability in magnitude of paleo-earthquakes revealed by trenching and historical records, along the Haiyuan Fault. Journal of Geophysical Research: Solid Earth 120: 8301-8333.

https://doi.org/ 10.1002/2015JB012163

[20] Meunier P, Hovius N, Haines JA (2008) Topographic site effects and the location of earthquake induced landslides. Earth. Planet. Sci. Lett. 275: 221-232. https://doi.org/10.1016/j.epsl.2008.07.020

[21] Meunier P, Uchida T, Hovius N (2013) Landslide patterns reveal the sources of large earthquakes. Earth and Planetary Science Letters 363: 27-33. https://doi.org/10.1016/j.epsl.2012.12.018

[22] Ningxia Longde County Local Chronicles Compilation Committee (1998) Longde County Records. Ningxia People Publishing House (in Chinese), Yinchuan

[23] Parker RN, Alexander LD, Nicholas JR, De Michele M, Li Y, Huang R, Whadcoat S, Petley DN (2011) Mass wasting triggered by the 2008 Wenchuan earthquake is greater than orogenic growth. Nature Geoscience 7: 449-452. https://doi.org/10.1038/ngeo1154

[24] Ren Z, Zhang Z, Chen T, Yan S, Yin J, Zhang P, Zheng W, Zhang H, Li C (2016) Clustering of offsets on the Haiyuan fault and their relationship to paleoearthquakes. GSA Bulletin 1-2: 3-18. https://doi.org/10.1130/B31155.1

[25] Seismological Bureau of Ningxia Hui Autonomous Region (1989) Summary of Ningxia Hui Autonomous Region historical earthquake record. Seismological Press (in Chinese), Beijing

[26] Tongwei County Annals Compilation Committee (1990) Tongwei County Records. Lanzhou University Publishing House (in Chinese), Lanzhou

[27] Wang L M, Shi Y C, Liu X (2003) Loess Dynamics. Seismological Press (in Chinese), Beijing

[28] Wang L, Wu Z, Xia K (2017) Effects of site conditions on earthquake ground motion and their applications in seismic design in loess region. Journal of Mountain Science 6: 1185-1193. https://doi.org/10.1007/s11629-016-3921-7

[29] Wells DL, Coppersmith KJ (1994) New empirical relationships among magnitude, rupture length, rupture width, rupture area, and surface displacement. Bull. Seism. Soc. Am. 84: 974-1002

[30] Wen XZ, Ma SL, Xu XW, He YN (2008) Historical pattern and behavior of earthquake ruptures along the eastern boundary of the Sichuan-Yunnan faulted-block, southwestern China. Physics of the Earth and Planetary Interiors. 1-2: 16-36. https://doi.org/10.1016/j.pepi.2008.04.013

[31] Xiji County Annals Compilation Committee (1995) Xiji County Records. Ningxia People Publishing House (in Chinese), Yinchuan

[32] Xu C, Xu XW (2014) The spatial distribution pattern of landslides triggered by the 2013 Lushan earthquake and its implication to the seismogenic blind-reverse-fault. Chin Sci Bull. 59:1416-1424. https://doi.org/10.1007/s11434-014-0202-0

[33] Xu YR, Du P, Li WQ, Zhang WH, Tian QJ, Xiong RW, Wang L (2020) Methods on historical earthquakes triggered landslides database mapping and its application- A case study on AD 1718 M 7.5 Tongwei earthquake. Chinese Journal of Geophysics (in Chinese) 63(3): 1235-1248. https://doi.org/ 10.6038/cjg2020N0146

[34] Xu YR, Zhang WH, Li WQ, He HL, Tian QJ (2018) Distribution characteristic of the AD 1556 Huaxian earthquake triggered disasters and its implications. Earthquake and Geology (in Chinese) 40(4): 721-737. https://doi.org/10.3969/j.issn.0253-4967.2018.04.001

[35] Xu X, Wen X, Yu G, Chen G, Klinger Y, Hubbard J, Shaw J (2009) Coseismic reverse-and oblique-slip surface faulting generated by the 2008 Mw 7.9 Wenchuan earthquake, China. Geology 37(6): 515-518. https://doi.org/10.1130/G25462A.1

[36] Xu Y, Allen MB, Zhang W, Li W, He H (2020) Landslide characteristics in the Loess Plateau, northern China. Geomorphology :107150. https://doi.org/10.1016/j.geomorph.2020.107150

[37] Yin YP, Wang FW, Sun P (2009) Landslide hazards triggered by the 2008 Wenchuan earthquake, Sichuan China. Landslides 6(2): 139-151. https://doi.org/10.1007/s10346-009-0148-5

[38] Yuan R M, Deng Q H, Cunningham D, Xu C, Xu XW, Chang CP (2013) Density distribution of landslides triggered by the 2008 Wenchuan earthquake and their relationships to peak ground acceleration. Bulletin of the Seismological Society of America 4: 2344-2355. https://doi.org/10.1785/0120110233

[39] Zhang PZ, Min W, Deng QD, Mao FY (2005) Paleoearthquake rupture behavior and recurrence of great earthquakes along the Haiyuan Fault, northwestern China. Science in China (Ser D) 48(3): 364-375. https://doi.org/10.1360/02yd0464

[40] Zhuang JQ, Peng JB, Xu C, Li Z, Densmore A, Milledge D, Iqbal J, Cui Y (2018) Distribution and characteristics of loess landslides triggered by the 1920 Haiyuan Earthquake, Northwest of China. Geomorphology 314: 1-12. https://doi.org/10.1016/j.geomorph.2018.04.012

Figure captions

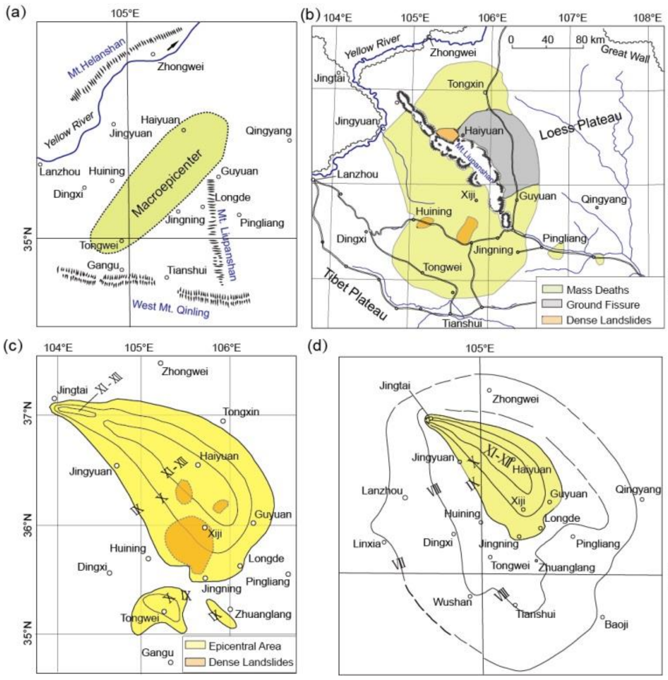

Fig.1 Maps of the epicentral area of the 1920 Haiyuan earthquake given by different studies. After the Haiyuan earthquake, (a) Dr. Weng, published their preliminary macro-epicentre area map of Haiyuan earthquake obtained after the first field scientific investigation; (b) Close et al (1922) published the map of earthquake damage by the International Disaster Relief Committee, after the field investigation in 1921; (c) The intensity distribution map given by Chinese scholars in the several scientific investigation during 1950s-1970s (Lanzhou Institute of Seismology, SSB, et al., 1980); (d) The intensity distribution map of the Haiyuan earthquake used since the 1980s (Department of Earthquake Disaster Prevention, SSB, 1995).

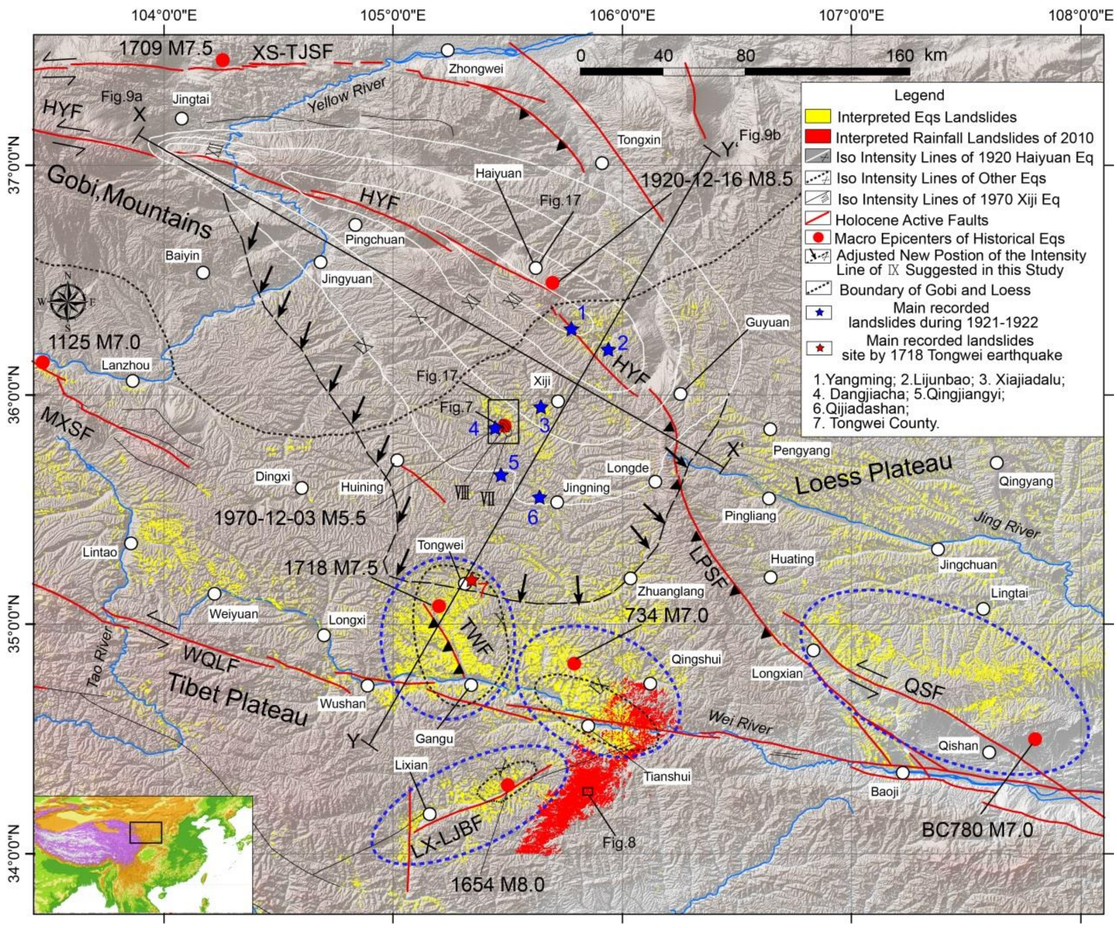

Fig.2 Distribution of interpreted landslides in the region around the Haiyuan, Tongwei, and other historical earthquakes, in the western part of the Loess Plateau, Northwestern China, shown over shaded relief. Faults: HYF: Haiyuan Fault; WQLF: West Qinling Fault; LPSF: Liupanshan Fault; TWF: Tongwei Fault; MXSF: Maxianshan Fault; LX-LJBF: Lixian- Luojiabao Fault; QSF: Qishan Fault. The thick black dashed line and black arrows denote the suggested new location of seismic intensity line Ⅸ in this study.

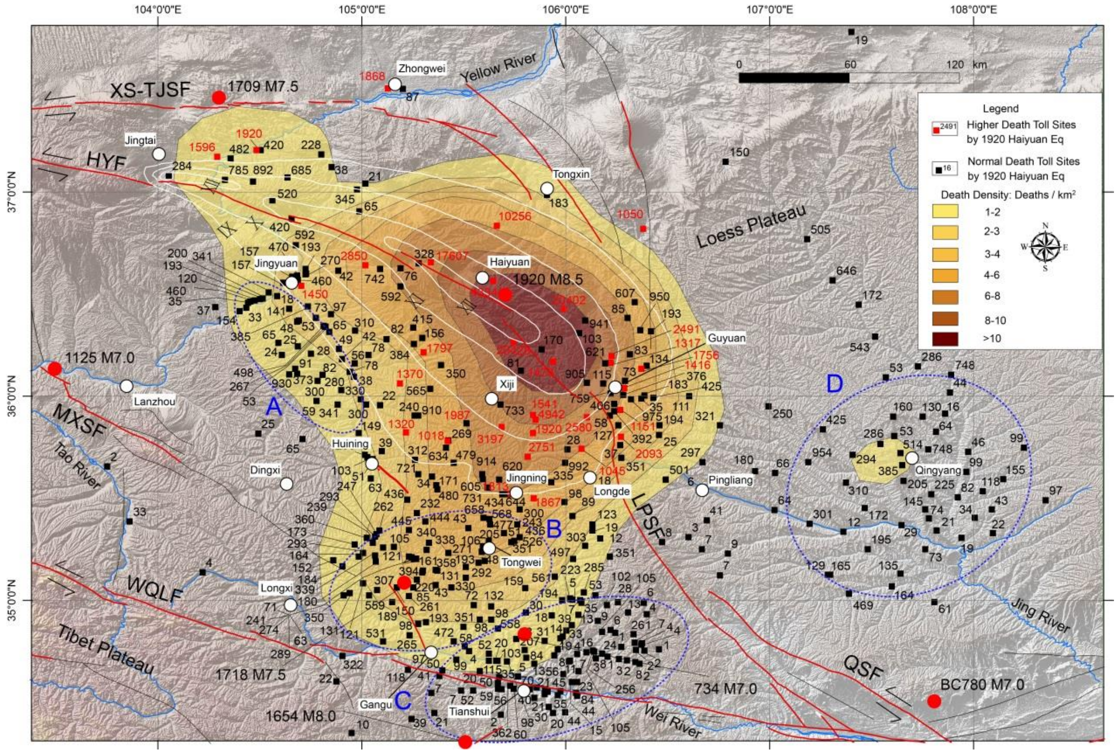

Fig. 3 Distribution map of township death tolls caused by the 1920 Haiyuan earthquake, shown over shaded relief. Haiyuan county suffered the most serious deaths. Most townships in it did not have specific statistical results, except Haiyuan county town with 4,234 deaths. The red rectangles show deaths ~10^3, the black rectangles show deaths ~10^2. The death density to the south Tongwei is 4~ deaths/ km^2, while the number can be up to ~20 deaths/ km^2 caused by the 1718 Tongwei earthquake. Region A (blue dashed ellipse) covers parts of the Jingyuan and Huining counties, which are located outside the intensity line Ⅸ, but the death toll is nearly equivalent to that within the nearby areas with intensity Ⅸ; Region B covers main parts of the Jingning, Tongwei and Gangu counties, which are located outside intensity line Ⅸ, and the death toll is relatively serious: the north part of the area with number of deaths mostly ~10^3 is larger than that the south part, at ~10^2; Region C covers Tianshui city and surrounding areas, the death toll in this region had decreases to ~10^2 or ~10^1; Region D covers Pingliang and Qingyang area. Although the death tolls in some towns are ~10^3, considering the relative higher population density, the death rate in this area is obviously reduced, and is similar to Region C. All numbers above are quoted from Lanzhou Institute of Seismology, SSB (1989) and Seismological Bureau of Ningxia Hui Autonomous Region (1989). See details in text.

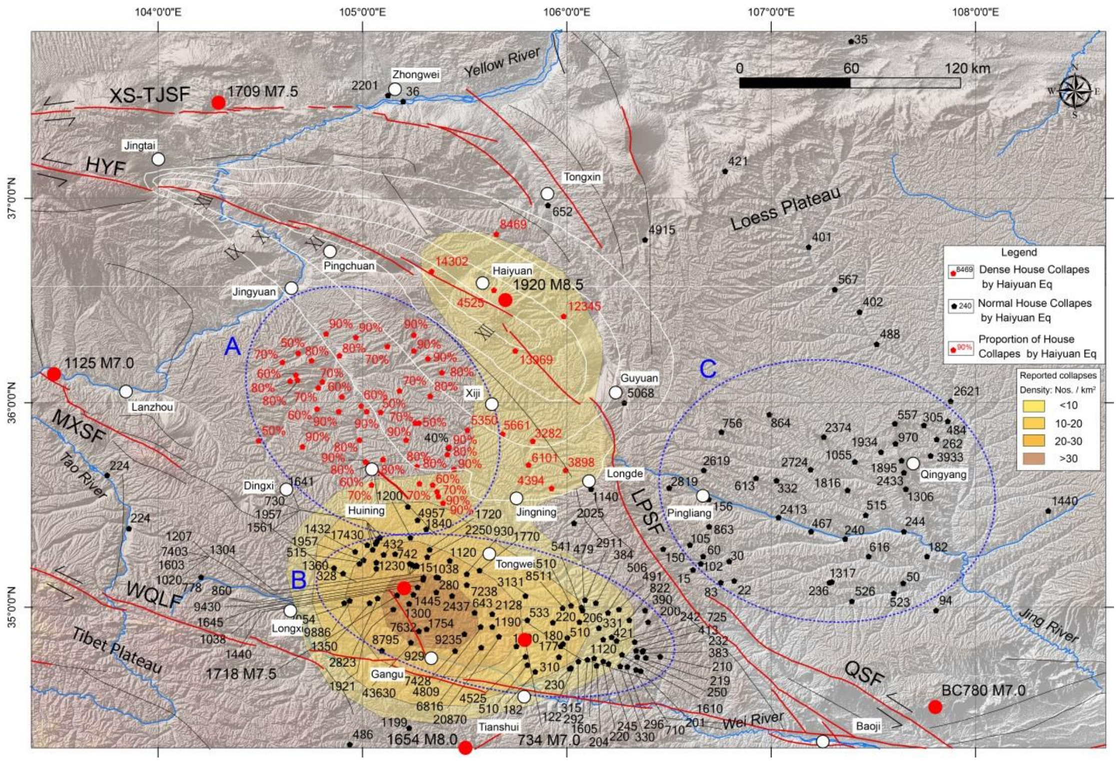

Fig.4 Distribution map of collapsed houses (including both conventional houses and loess caves) caused by the 1920 Haiyuan earthquake, shown over shaded relief. Although Haiyuan county suffered heavy fatalities, most townships in it did not have specific data for collapsed houses, so the collapse density appears smaller than would be expected from the death toll (Fig. 3). Available data for Region A is expressed in collapse rate rather than absolute numbers, and so is not contoured for density. Note that collapse rate of 50%-90% outside intensity line Ⅸ is similar to the range within intensity line Ⅸ, of 60-90% Region B shows the apparently high number of collapsed houses around Tongwei (see text). Region C covers the area between Pingliang and Qingyang; although individual counts are high, the regional density is low. All numbers above are quoted from Lanzhou Institute of Seismology, SSB (1989) and Seismological Bureau of Ningxia Hui Autonomous Region (1989).

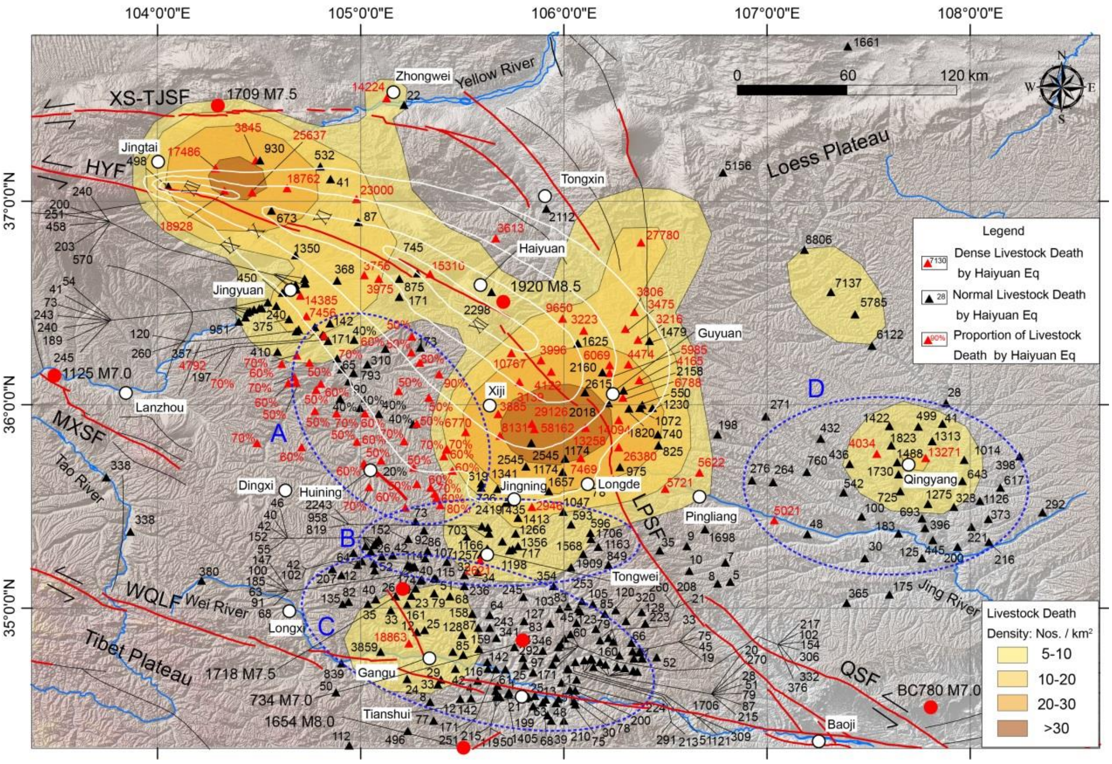

Fig.5 Distribution map of large livestock death tolls caused by the 1920 Haiyuan earthquake, shown over shaded relief. Haiyuan County suffered the most serious deaths; although there are not detailed livestock data, the distribution is consistent with the human death toll. There are two dense centres; one is located near Jingtai along the Yellow River valley, another is located in Xiji-Guyuan-Jingning counties. Region A covers parts of Jingyuan, Xiji and Huining counties, where the death rate of 50%-80% outside the intensity of Ⅸ is similar to value within intensity line Ⅸ of 50-70%, and intensity line Ⅹ of 50-90%. Region B covers the number of large livestock deaths in the order of $\sim 10^3$ at each site; Region C covers the number of the large livestock deaths on the order of $\sim 10^2$, which gradually decreases from north to south. Region D has values of $\sim 10^3$; some of the higher numbers reflect the towns with relative higher populations, rather than the real rate which is different with Region A and Region B. All numbers above are quoted from Lanzhou Institute of Seismology, SSB (1989) and Seismological Bureau of Ningxia Hui Autonomous Region (1989). See details in text.

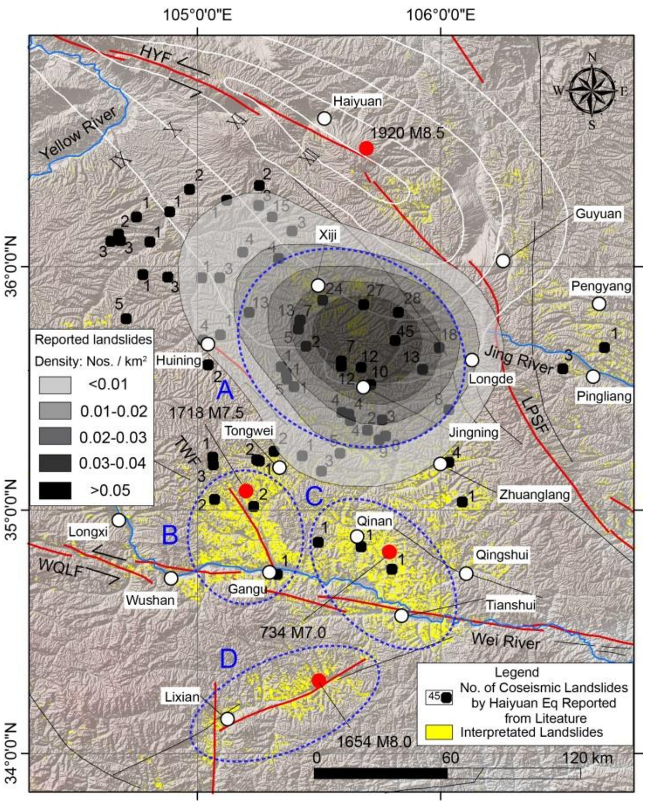

Fig. 6 Distribution map of recorded coseismic landslides triggered by the 1920 Haiyuan earthquake, shown over shaded relief. After the Haiyuan earthquake, the reported number of "Cracked Mountains and Valleys" was the highest to the south of the Haiyuan Fault. The dense region is around Xiji, Huining, and Jingning counties (Region A). There are several records in the northwest of Region A to the east of the Yellow River. There are also reports around Tongwei county. There are only 5 reported landslides in Region B; landslides in this area were likely to have been triggered by 1718 Tongwei earthquake. Only 3 landslides were reported in Region C, where majority of landslides are likely to have been triggered by AD 734 Tianshui earthquake. No reported landsliding was caused by the Haiyuan earthquake in Region D; landslides in this area are likely to have been triggered by the AD 1654 Lixian earthquake. All numbers above are quoted from Lanzhou Institute of Seismology, SSB (1989) and Seismological Bureau of Ningxia Hui Autonomous Region (1989). See details in text.

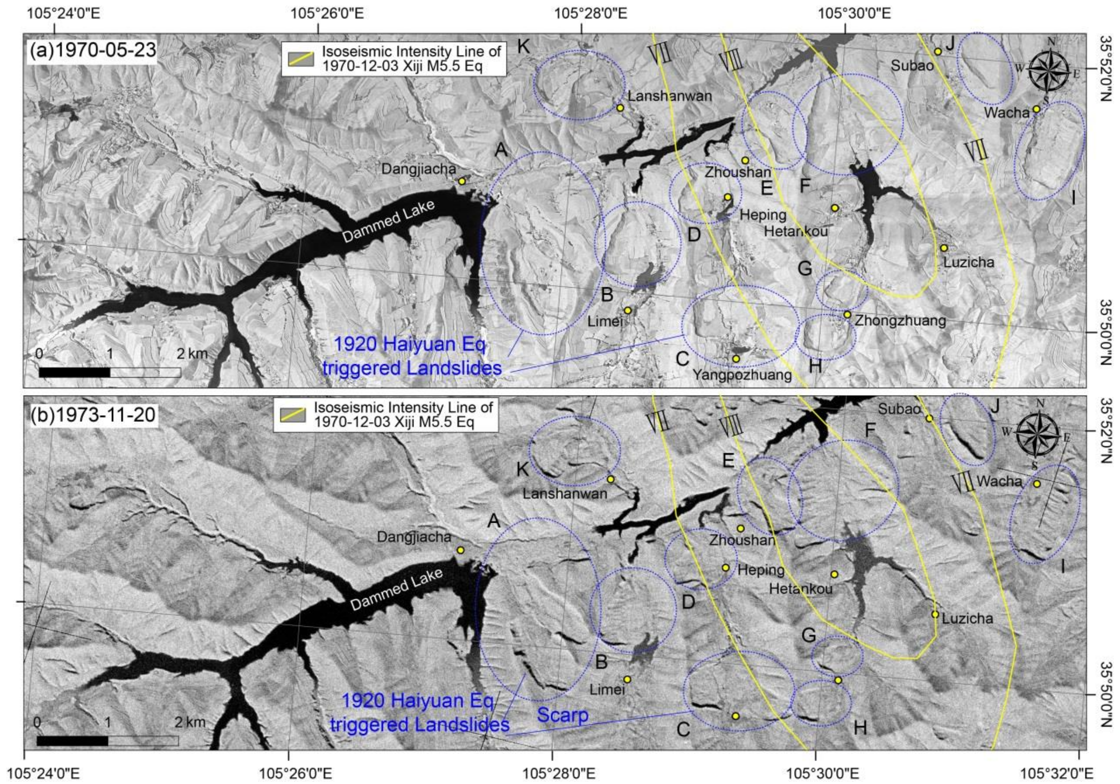

Fig. 7 Comparison of landslides and dammed lakes before (a) and after (b) the M 5.5 Xiji earthquake on 3 December, 1970, in KeyHole images. The image (a), taken 7 months before the 1970 Xiji earthquake, shows that the "dammed lake" (local name “Shuiyan”) near Luzicha already existed at that time, and that it was formed by Landslide F with a clear trailing scarp. No significant new slip was observed in Landslide F after the Xiji earthquake; (b) Landslides G and H in the same valley also existed before the Xiji earthquake. Similarly, Landslide A was triggered by 1920 Haiyuan earthquake, not the Xiji earthquake, and led to the formation of the Dangjiacha earthquake dammed lake (Lanzhou Institute of Seismology, SSB, 1989); Landslide B formed another dammed lake, but which dried up before our fieldwork survey in 2018. Dense landslides formed a series of dammed lakes along the river valley, such as those adjacent to Landslides A, B, D, E, J, etc. Landslides located at the head of valleys do not easily form dammed lakes, such as Landslides C, H, G, K, etc. Even though some landslides have been modified to varying degrees, the overall shape can be identified 50 and 100 years after the Haiyuan earthquake, within intensity line Ⅹ of the Xiji earthquake. See details in text.

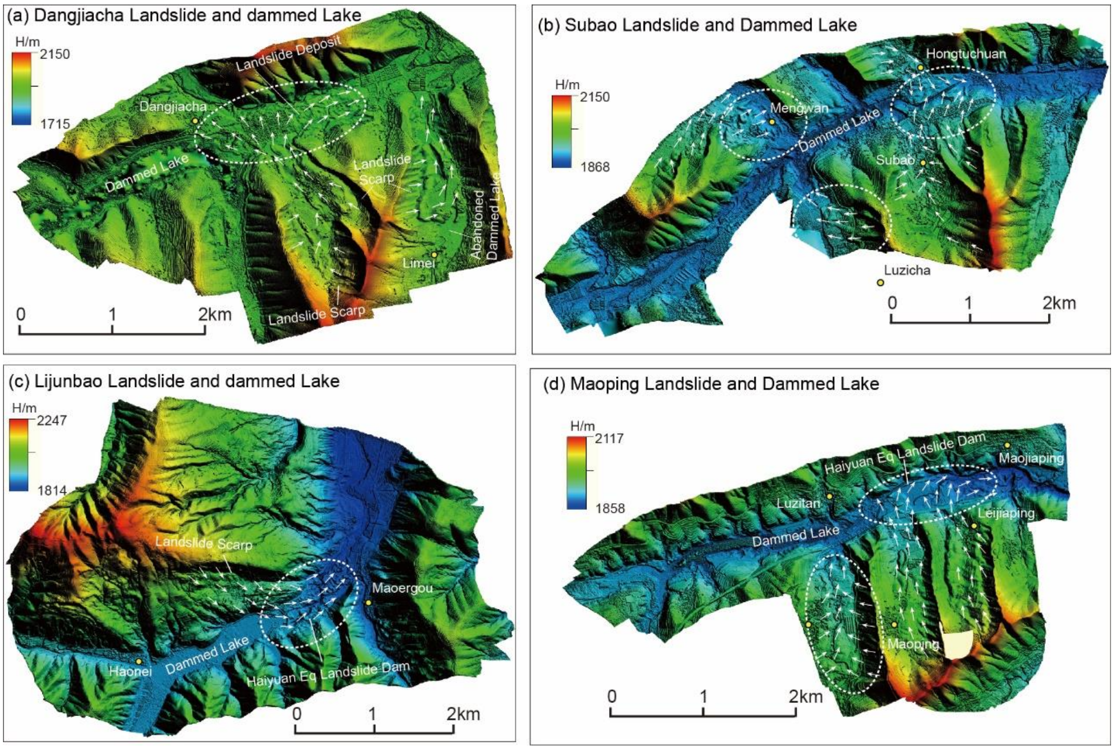

Fig. 8 UAV-DEMs showing representative landslides and related dammed lakes caused by the 1920 Haiyuan earthquake in Xiji county (a) 35.842665°N, 105.461245°E, The Dangjiacha Landslide blocked the river valley, forming the largest dammed lake; (b) 35.868602°N, 105.510885°E, the dammed lake in Subao town (since changed name to Zhenhu town for tourism development, meaning dammed lake) is formed by the Subao Landslide on the south side and the Hongtuchuan Landslide on the north side. A diversion channel has been opened on the landslide body, but the lake still exists. Most of the smaller dammed lakes in the western branch of Subao have dried up; (c) 36.197216°N, 105.863743°E, LiJunbao dammed lake is formed by the landslide on the north side. After the earthquake, the local residents excavated the flood discharge channel, the water storage level was 10~ m, but the coverage area was large with several km^2; (d) 35.878668°N, 105.559454°E, the dammed lake is formed by the co-seismic landslide material from the two branch valleys near Maoping village.

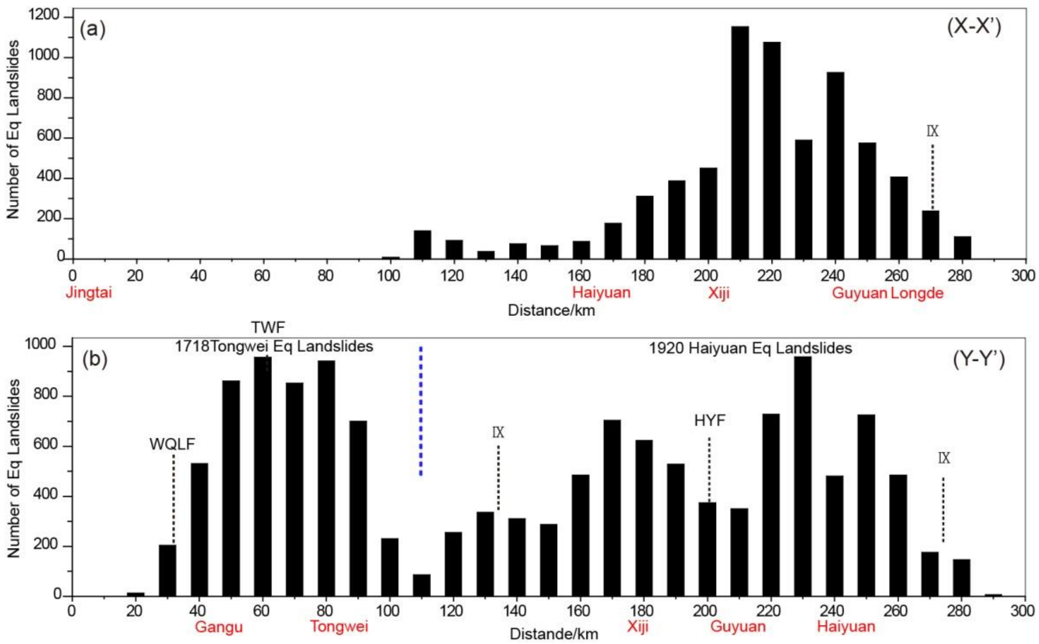

Fig. 9 Spatial distribution of earthquake triggered landslides projected along profiles parallel (X-X') and perpendicular (Y-Y') to the Haiyuan fault. See location in Fig. 2

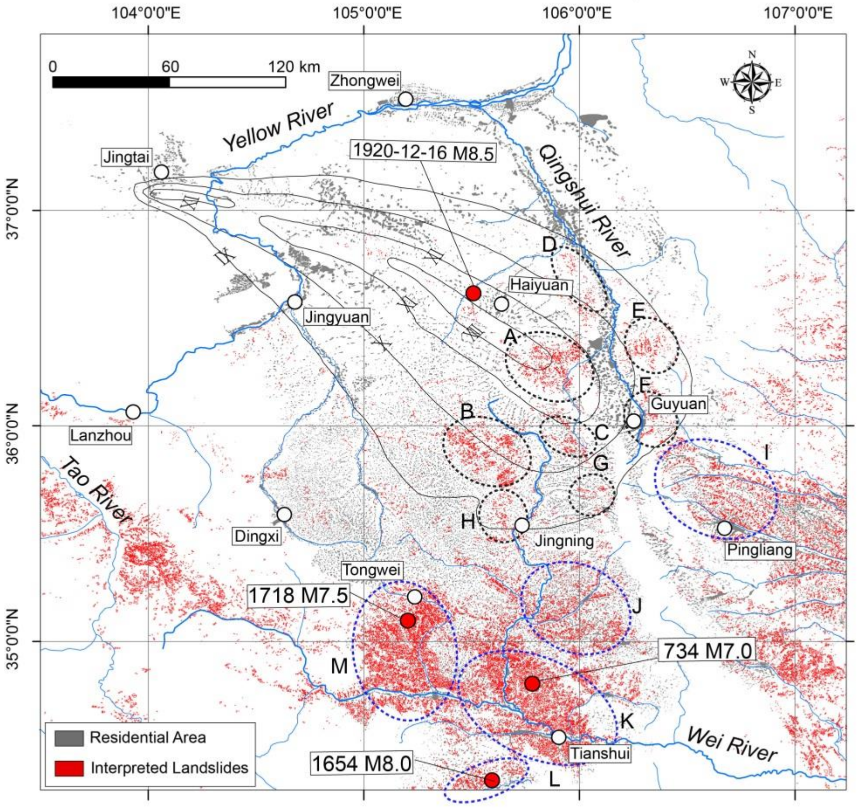

Fig. 10 Distribution map of the settlements and landslides triggered by historical earthquake. Regions with dense landslides are outlined by black thick dashed lines. Regions A-I are related to 1920 Haiyuan earthquake, Region J is possibly related to 1352 Dingxi earthquake, Regions K, L, M are related to 734 Tianshui earthquake, 1718 Tongwei earthquake and 1654 Lixian earthquake, respectively. Among them, Region A spans the Haiyuan Fault with dense landslides but the settlements are relatively sparse. Regions D-F are located on the northeast side of the Haiyuan fault; the sparse settlements are mostly concentrated in river valleys. During the earthquake, people died mainly due to house collapsed rather than landsliding. Only some of the settlements in the Regions A-H were damaged by landslides. Regions C and G are located on the southwest side of the Haiyuan Fault, with the densely landslides and settlements, so the people death may have related to landsliding. Regions B and H south of Xiji and Jingning Counties, respectively. experienced the most serious damage to settlements. See the text for details.

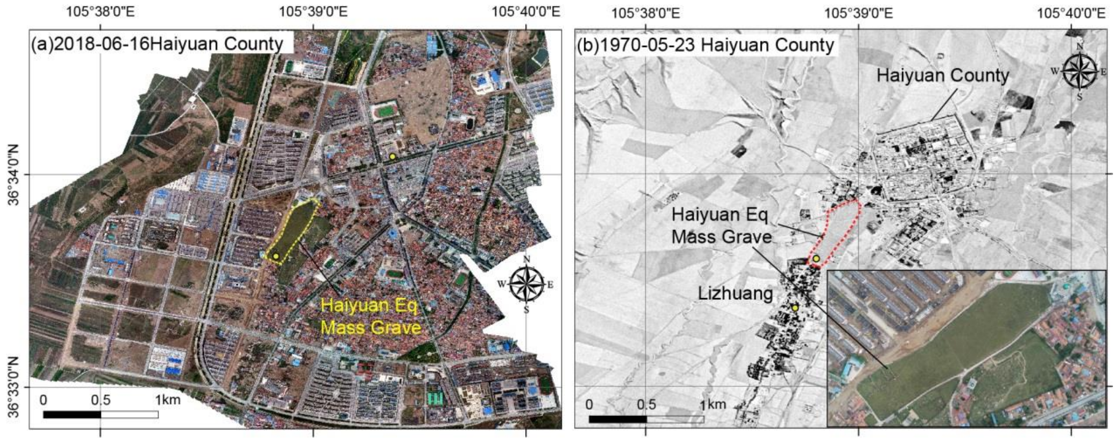

Fig. 11 Comparison of satellite imagery of the Haiyuan township in 2018 (98 years after the 1920 Haiyuan Earthquake) (a) and KeyHole image in 1970 (50 years after the earthquake) (b). Inset photo shows the Hui mass grave from the Haiyuan earthquake. This site was located in a southwestern suburb at the time of the earthquake, but is now surrounded by new buildings. Urban expansion has led to new buildings with reinforced-cement structure, but traditional houses without any reinforcement remain within the old township. It means that when the next strong shaking happens, the devastation will be similar or worse than in 1920.

Fig. 12 Field photos show abandoned and occupied houses and loess caves (yaodong) in rural villages. (a) Dangjiacha village (35.837003°N, 105.462855°E) at the Dangjiacha landslide body triggered by the Haiyuan earthquake. The village was rebuilt after the event, see location in Fig.7. (b). Houses rebuilt in Dangjiacha village without frame structures. The walls were rebuilt by rammed earth at the bottom, and by non-sintered bricks at the top, which are easily damaged by strong shaking. (c) Some of new and rebuilt houses used sintered bricks, but without reinforced columns, in Xiji county. (d) A rebuilt house without frame structure, which used prefabricated panels instead of a reinforced cast-in-place build. This technique saves money, but has the very weak shock-resistance of the houses destroyed by the Haiyuan earthquake. (e) and (f) Photos showing the abandoned caves (yaodong) along the Haiyuan Fault (36.626165°N, 105.367362°E) at Haiyuan county. The destroyed houses and yaodong were all abandoned.

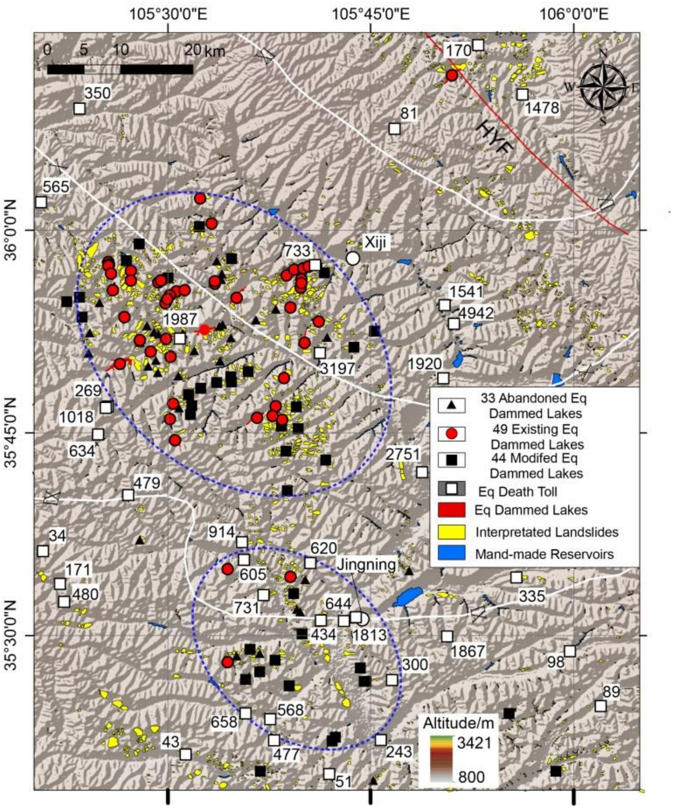

Fig. 13 Distribution map of landslides and dammed lakes triggered by the 1920 Haiyuan earthquake, shown over shaded relief. Blue dashed ovals highlight regions with dense landslides triggered by the earthquake. Dammed lakes formed by landslides are located along river valleys, and are classified as existing (i.e. lake is still present), abandoned (lake silted up or drained) or modified (in use as reservoirs, buttressed by man-made dams).

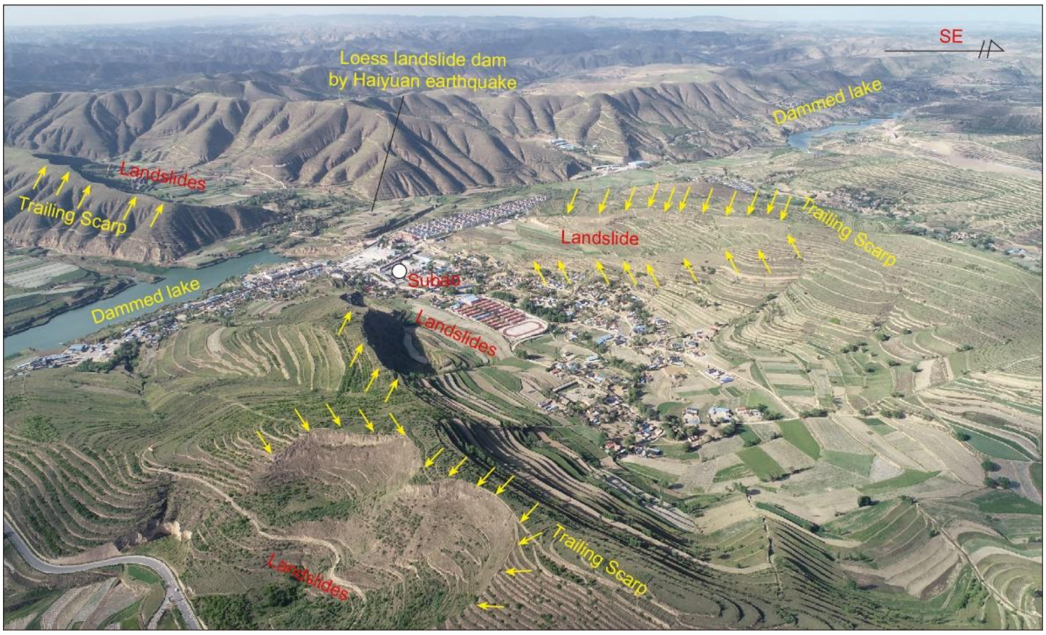

Fig. 14 Several loess landslides triggered by Haiyuan earthquake at Subao (35.861545°N, 105.507538°E). Some landslides blocked the river valley and formed the loess dams and dammed lakes. The lakes are shallow. The shape of dams can be changed by local people for farming. See location at Fig.8b.

Table Captions

Table 1 Characteristics of major earthquakes and rainfall landslides in and around the Loess Plateau, China

Date	Events	Lon/Lat	Intensity	Deaths	Total No.	Ref.
1718-06-19	Tongwei *M* 7.5	35.08°N, 105.20°E	X	>70,000	5,019	Xu et al. 2020
1920-12-16	Haiyuan *M* 7.8-8.5	36.50°N, 105.70°E	XII	>234,000	7,151	This study
2008-05-12	Wenchuan M_w 7.9	31.01°N, 103.42°E	XI	>87,150	52,194	Du et al., 2020

2010-08-12	Tianshui Rainfall	34.33°N，105.75°E	-	4	53,913	Xu et al., 2020

Table 2 List of death tolls of the main counties affected by the 1920 Haiyuan earthquake

Subarea	No.	Counties	Death*	Death**	Death***	Death****	Death*****	County Town Death**
Epicenter	1	**Haiyuan**	**>45,000**	**73,030**	**73,027**	**73,604**	**73,604**	**4,334**
	2	**Guyuan**	**>36,000**	**40,176**	**39,176**	**36,176**	**39,068**	**376**
	3	Longde	**>10,000**	**28,370**	**21,304**	**21,732**	**21,341**	18

Subarea	No.	Counties	Death*	Death**	Death***	Death****	Death*****	County Town Death**
	4	Jingning	**>32,000**	**12,447**	**9,619**	**12,447**	**12,447**	**1,813**
	5	Huining	**>30,000**	**13,962**	**13,938**	**13,742**	**13,942**	51
	6	Jingyuan	**>20,000**	**31,933**	**31,591**	**31,933**	**22,930**	**1,920**
	7	**Tongwei**	**>20,000**	**18,108**	**10,206**	**10,206**	**28,100**	**241**
North of HYF	8	Tongxin	>15,000	2,558	3,101	-	-	183
	9	Zhongwei	>700	-	87	-	-	-
	10	Zhuanglang	>1,000	5,376	5,376	-	-	-
	11	Qin'an	>10000	3,134	-	-	-	-
	12	Dingxi	>4,200	1,200	-	-	-	-
South of HYF	13	Tianshui	>4,600	-	2,829	-	-	127
	14	**Gangu**	>2,500	-	**1,363**	-	-	**97**
	15	Qingshui	>1,400	1,480	1,483	-	-	66
	16	Wushan	384	-	322	-	-	-
	17	Jingchuan	>5,000	7,10	-	-	-	-
	18	Qingyang	>4,000	2,405	2,405	-	-	44
	19	Ningxian	>4,000	1,231	1,212	-	-	-
East of LPS	20	Pingliang	>3,000	1,311	909	-	-	64
	21	Zhenyuan	>3,000	2,895	3,005	-	-	-
	22	**Huanxian**	>3,000	2,016	2,016	-	-	**646**
	23	Lingtai	>1,000	1,127	1,196	-	-	-

*From China Daily, published in March 1921, 3 months after the Haiyuan earthquake; ** From Chinese Agricultural & Business Bulletin, published in August 1921, 8 months after the Haiyuan earthquake; *** From Dr. Xie Jiarong et al., Reports of 1920 Gansu (Haiyuan) earthquake, published after the field investigation, October 1921, 10 months after the Haiyuan earthquake; **** From Chinese Geoscience Magazine, published in 1922, more than 12 months after the Haiyuan earthquake. All numbers above are quoted from LIS, SSB (1989) and SBNHAR (1989). ***** From corresponding county records, published during 1990s, more than 70 years after the Haiyuan earthquake. Tongwei's deaths toll from Tongwei county annals compilation committee (1990) includes the earthquake shaking deaths and later starvation and freezing deaths, which is much bigger than previous numbers.

Table 3 Structure of statistical table of disaster situation in the Haiyuan earthquake in Chinese

County townships	Earthquake numbers	Casualties		Dead livestock	Loss of property		"Cracked mountains"
		Death	Injury		Houses	Caves	
Haiyuan		4,334		2,298	3,481	1,044	
Longde	17	18		98	1,140	-	
Jingning	110	1,813		1,435	-	-	
Huining	~300	51		20%	60%		

Guyuan		376	84	550	1,433	
Jingyuan	489	1,920		3,845		1
Tongwei		241	166	185	7,403	
Gangu	~20	97		-	292	1
Tianshui		127		114		
Mengxuanbao		2,195		6,770	695	24

Data from Lanzhou Institute of Seismology, SSB (1989) and Seismological Bureau of Ningxia Hui Autonomous Region (1989)

Table 4 Records of Earthquake disasters between Tongwei and Gangu County

Place	Event	Description Content	References
Tongwei	1718	A great earthquake happened, mountain landsliding, the Mt. Bijia's peak collapsed and disappeared, ground cracked at the valley flat floor, the disaster is more serious in the south part, there are many triggered landslides around it,	Lanzhou Institute of Seismology, SSB, 1989

		which **killed >40,000 urban and rural people in all**. Because of northeast township collapsed, the County government moved to the west part after the earthquake, **10 yrs. later it transferred to new place in 1728**, another 7 yrs later, the government was ordered to restore the new rebuilding township in 1735.
	1920	10,206 people died in the County, among them **West part was hardest hit with 4,029 death**, >50,000 houses collapsed, east part and south part both with 1,600 death, respectively, the township just with just 375 people death.
Gangu	1718	The earthquake hit the whole county area, the northern mountains moved southward and buried the old Yongning Town; Lixin Town left less than half, there were no survivors of residents in the northwest area, **killed >30,000 local people**. The earthquake caused extensive landsliding within 50 km, in all the Gangu County is buried underground.
	1920	**Only 1,365 people died in the County**, West and North of the county with 362, 398 deaths, respectively, South of the county just had 90 deaths, while the County township just decreased to 12 deaths. More than 50,000 houses (loess caves) collapsed.

Table 5 List of deaths within main landslide regions of the Haiyuan Earthquake

No.	Landslide region	Number of landslides	Death toll
1	Region A	1,480	1,729

2	Region B	1,102	5,917
3	Region C	400	9,063
4	Region D	497	-
5	Region E	400	3,918
6	Region F	900	1,835
7	Region G	347	8,009
8	Region H	150	2,083
Total		5,276 (73.7%)	32,554 (13.9%)